doi: 10.12029/gc20201124002

刘宝山,张春鹏,程招勋,寇林林,李成禄,韩仁萍. 2023. 黑龙江争光大型金矿成矿流体He-Ar-S同位素组成及成矿流体来源的示踪[J]. 中国地质, 50(3): 952-961.

Liu Baoshan, Zhang Chunpeng, Cheng Zhaoxun, Kou Linlin, Li Chenglu, Han Renping. 2023. Source teacing and He-Ar-S isotopic compositions of ore-forming fluid in the Zhengguang large gold deposit, Heilongjiang Province[J]. Geology in China, 50(3): 952-961(in Chinese with English abstract).

黑龙江争光大型金矿成矿流体He-Ar-S同位素组成及成矿流体来源的示踪

刘宝山[1],张春鹏[1],程招勋[2],寇林林[1],李成禄[2],韩仁萍[1]

(1. 中国地质调查局沈阳地质调查中心,辽宁 沈阳 110034;2. 黑龙江省自然资源调查院,黑龙江 哈尔滨 150036)

提要:【研究目的】黑龙江争光金矿床位于兴安地块东缘嫩江—黑河北东向断裂带西北侧的奥陶纪多宝山岛弧带上。本文通过对主成矿期的矿石样品研究,探讨了成矿流体的来源。**【研究方法】**选择9件主成矿期的黄铁矿和方铅矿进行了系统研究,测定了He、Ar和S同位素组成。**【研究结果】**其含金石英脉中黄铁矿和方铅矿的流体包裹体$^{3}He/^{4}He=1.95\times10^{-6}$~$5.03\times10^{-6}$,$^{40}Ar/^{36}Ar=349.1$~$453.9$。幔源He占13.17%~44.67%,平均27.58%,显示了成矿流体以大气降水为主,但同时有地幔流体成分,表明金矿床成矿作用与地幔活动有着密切的关系。矿物$\delta^{34}S=-1.2‰$~$-3.9‰$,平均$-2.33‰$,可能来自深源地幔流体,但其中有地壳流体的加入。**【结论】**洋壳向兴安地块俯冲,俯冲流体交代地幔楔发生部分熔融,流体上升至地表浅部与下渗的大气降水混合形成成矿流体,由于温度和压力的下降和流体沸腾作用导致成矿流体物理化学条件的改变,从而使成矿物质沉淀。

关　键　词: He-Ar-S同位素;壳幔相互作用;争光大型金矿;地质调查工程;大兴安岭

创　新　点:壳幔相互作用幔源流体的加入是争光金矿成矿的重要条件,为该地区金矿成因的探讨提供了参考。

中图分类号:P597; P599　　**文献标志码:**A　　**文章编号:**1000-3657(2023)03-0952-10

Source teacing and He-Ar-S isotopic compositions of ore-forming fluid in the Zhengguang large gold deposit, Heilongjiang Province

LIU Baoshan[1], ZHANG Chunpeng[1], CHENG Zhaoxun[2], KOU Linlin[1], LI Chenglu[2], HAN Renping[1]

(1. *Shenyang Center, China Geological Survey, Shenyang* 110034*, Liaoning, China;* 2. *Heilongjiang Institute of Natural Resources, Harbin* 150036*, Heilongjiang, China*)

Abstract: This paper is the result of geological survey engineering.

[Objective] Zhengguang gold deposit in Heilongjiang Province is located in the Ordovician Duobaoshan island arc belt on the northwest side of Nenjiang—Heihe NE trending fault zone in the eastern margin of Xing'an block. By study of the ore samples in

收稿日期: 2020-11-24;**改回日期**: 2021-07-19

基金项目: 国家重点研发计划课题典型矿集区三维地质结构与矿体定位(2017YFC0601305),中国地质调查局地质调查项目(DD20190156)联合资助。

作者简介: 刘宝山,男,1970年生,教授级高级工程师,主要从事地质矿产调查工作;E-mail: liubaoshan1111@163.com。

通讯作者: 寇林林,女,1983年生,教授级高级工程师,主要从事矿产综合研究工作;E-mail: koulinlin@126.com。

the main metallogenic period, we aim to explore the source of ore-forming fluids. **[Methods]** Nine ore samples from the main metallogenic stage were selected for systematic study of the He, Ar and S isotopic compositions. **[Results]** The results show that the $^{3}He/^{4}He$ and $^{40}Ar/^{36}Ar$ ratios for fluid inclusions of pyrite and galena in the gold-bearing quartz veins are 1.95×10^{-6}-5.03×10^{-6} and 349.1-453.9, respectively. The mantle-derived He accounting for 13.17%-44.67%, averagely 27.58%, indicating that the metallogenic fluid is mainly atmospheric precipitation, with the composition of mantle fluid as well, reflecting that the mineralization of gold deposit is closely related to mantle activity. The $\delta^{34}S$ of minerals is-1.2‰ - -3.9‰, averagely -2.33‰, probably from deep mantle fluid, also with the addition of crustal fluid. **[Conclusions]** The oceanic crust subducted toward Xing'an block, with mantle wedge metasomatized by the subducted fluid, and resulted in partial melting and fluid rising to the shallow surface mixed with the downward precipitation to form the metallogenic fluids. The decrease of temperature and pressure and fluid boiling lead to the change of physical and chemical conditions of the metallogenic fluids and precipitate metallogenic materials.

Key words: He- Ar- S isotopic composition; crust- mantle interaction; Zhengguang large gold deposit; mineral exploration engineering; Greater Khingan Mountains

Highlights: Crust- mantle interaction and subsequent injection of mantle-derived fluids have played an important role in Zhengguang gold mineralization, which provides a reference for discussion of the genesis of gold deposits in this area.

About the first author: LIU Baoshan, male, born in 1970, professor level senior engineer, mainly engaged in mineral geological survey; E-mail: liubaoshan1111@163.com.

About the corresponding author: KOU Linlin, female, born in 1983, professor level senior engineer, mainly engaged in mineral research; E-mail: koulinlin@126.com.

Fund support: Supported by the National Key Research and Development Program of China (No.2017YFC0601305) and the project of China Geological Survey (No.DD20190156).

1　引　言

争光金矿位于兴安地块大兴安岭北段,是嫩江地区继多宝山大型铜矿之后发现的大型金矿床,金金属量(331+332+333)达到23 t,平均品位为3.25 g/t(黑龙江省齐齐哈尔矿产勘察开发总院, 2009),该矿床以其独特的成矿地质背景和较高的金储量引起了国内外矿床学研究者的关注。前人对其地质特征进行了初步研究,赵广江等(2007)认为争光金矿床属构造蚀变岩型;邓轲等(2013)据流体包裹体研究认为争光金矿床是低硫型浅成低温热液矿床;佟匡胤等(2015)通过对争光金矿床赋矿围岩、控矿构造、矿体产状、主成矿温度、流体包裹体等多方面对比研究,也认为该矿床成因属于浅成低温热液型。宋国学等(2015)综合含金脉系特征、矿物组合、蚀变类型、闪锌矿Fe含量等,明确提出争光金矿床为中硫型浅成低温热液型。武子玉等(2006)根据$\delta^{18}O$-δD图解中成矿流体的投影点位于大气降水与岩浆水之间和碳、硫同位素具有地幔的特征,得出成矿流体为大气降水、变质水和岩浆水的混合水的结论,并认为争光金矿为热液-构造蚀变岩型。因此,争光金矿床成矿物质来源和成矿机制仍需要进一步探讨。近年来,惰性气体同位素体系被广泛应用于成矿物质和成矿过程的示踪研究,取得了许多其他方法无法获得的重要信息(曾志刚等,2000;Winckler et al., 2001;Ballentine et al., 2002;Mao et al., 2002, 2003;Moreir et al., 2003;薛春纪等, 2003; 孙晓明等, 2006),其主要原因在于惰性气体同位素体系在水/岩反应中基本保持不变,同时不同来源的成矿流体惰性气体同位素组成差异甚大,可以反映成矿流体来源和演化过程的原始信息。因此,本文在黄铁矿和方铅矿流体包裹体研究的基础上,进一步研究了成矿流体的氦、氩、硫同位素特征,进一步讨论成矿流体的来源并为矿床的成因提供新的依据。

2　矿床地质概况

矿区位于兴安地块东缘嫩江—黑河北东向断裂带西北侧,区域断裂构造发育,以压性、压扭性断裂和断裂破碎带为主, NW向三矿沟—多宝山—裸河断裂带和区内NW向的多宝山复式褶皱背斜轴部相复合,为矿集区基础构造,控制了古生代早奥陶世多宝山铜钼、铜山铜钼、争光金等矿床的空间分

布(赵广江等, 2006)。

矿区出露地层主要为中奥陶统铜山组和多宝山组。铜山组为安山质凝灰岩和砂质板岩夹大理岩;多宝山组以安山质凝灰岩、凝灰质砂岩、安山岩为主,夹炭质板岩和薄层火山角砾岩,是主要的赋矿围岩。构造主要有NW向、NE向和NNE向断裂,NE向断裂截切NW向断裂,并控制了金矿体的产出(赵广江等, 2006, 2007)。出露的侵入岩主要为闪长岩,有少量闪长玢岩、花岗细晶岩、花岗斑岩、煌斑岩等脉岩产出,均侵入于多宝山组火山岩。闪长岩体呈不规则椭圆状岩株沿NE向与NW向断裂交汇部位侵入,地表出露面积约1.8 km^2(图1)。

矿带多沿NW向与NE向断裂的交汇部位产出,控制矿体空间产出的构造主要为接触带构造,其次为与NW向向斜轴面近直交的NE向张性断裂构造、节理构造等(高荣臻等,2015),至2018年已发现控制金矿体176条(晁温馨,2018)。

金矿脉主要分布在多宝山组含砾凝灰岩、安山岩、构造破碎带及闪长岩与多宝山组的内外接触带中,其矿石类型主要是以黄铁矿、方铅矿、闪锌矿含金石英网脉型为主,其次是黄铁矿、方铅矿、闪锌矿、黄铜矿含金安山岩、凝灰岩型。矿石中金属硫化物主要为黄铁矿、闪锌矿、方铅矿、黄铜矿(图2),少量黝铜矿、辉银矿、斑铜矿、辉钼矿、蓝铜矿、自然

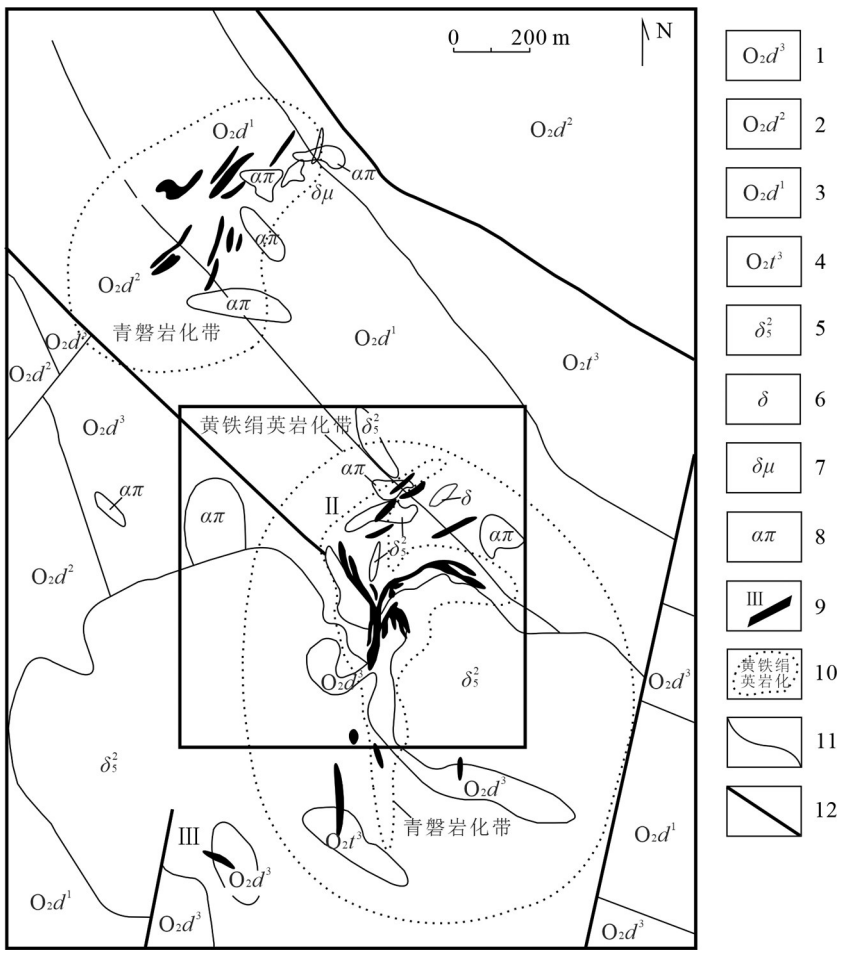

图1 黑龙江争光矿区地质图(据黑龙江齐齐哈尔矿产勘查开发总院, 2009修改)

1—多宝山组三段;2—多宝山组二段;3—多宝山组一段;4—铜山组三段;5—闪长岩体;6—闪长岩脉;7—闪长玢岩;8—次安山岩;9—矿带及编号;10—蚀变带界线;11—地质界线;12—断裂

Fig.1 Geological map of the Zhengguang gold deposit in Heilongjiang (modified from Heilongjiang Institute of Natural Resources, 2009)

1−3rd member of Duobaoshan Formation; 2−2nd member of Duobaoshan Formation; 3−1st member of Duobaoshan Formation; 4−3rd member of Tongshan Formation; 5−Diorite pluton; 6−Diorite vein; 7−Diorite porphyrite; 8−Secondary andesite; 9−Ore zone and number; 10−Alteration zone boundary; 11−Geological boundary; 12−Fracture

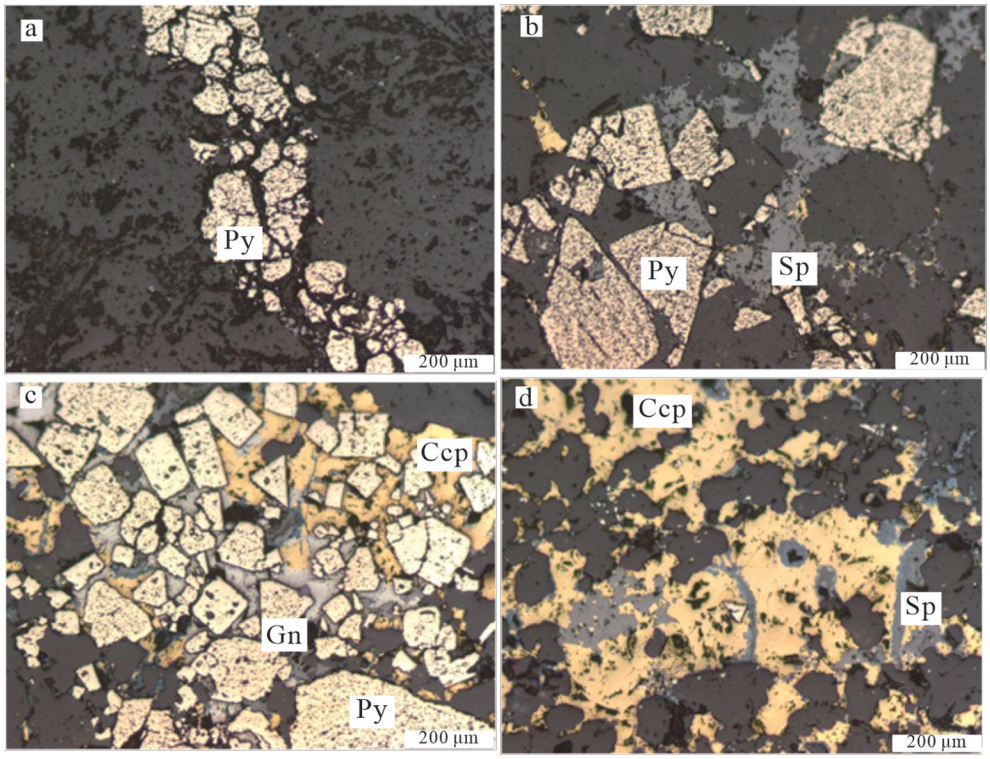

图2 争光矿区主要金属矿物及矿石组构镜下特征

a—脉状黄铁矿;b—闪锌矿交代早期自形黄铁矿;c—黄铜矿、方铅矿交代早期自形黄铁矿;d—脉状闪锌矿交代黄铜矿;Py—黄铁矿;Sp—闪锌矿;Ccp—黄铜矿;Gn—方铅矿

Fig.2 Micrograghs for the characteristics of metallic minerals and ores in the Zhengguang gold deposit

a-Veined pyrite; b-Sphalerite metasomatized early automorphic pyrite; c-Chalcopyrite and galena metasomatized early automorphic pyrite; d-Vein sphalerite metasomatized chalcopyrite; Py—Pyrite; Sp—Sphalerite; Ccp—Chalcopyrite; Gn—Galena

金等,其中黄铁矿、闪锌矿及石英为主要的载金矿物(赵广江等,2007;付艳丽和杨言辰,2010;邓轲等,2013;高荣臻等,2015)。矿石结构主要有自形—半自形粒状结构、他形粒状结构、乳滴结构和压碎结构。矿石构造主要为浸染状和细脉状,其次为条带状、角砾状、块状等构造(图3)。成矿阶段划分为石英-黄铁矿Ⅰ阶段、黄铁矿-黄铜矿-方铅矿-闪锌矿多金属硫化物Ⅱ阶段、碳酸盐Ⅲ阶段(晁温馨, 2018)。

3 样品分析方法

用于研究的9个样品为采自争光金矿Ⅱ号矿体含金石英脉中的黄铁矿和方铅矿,为了对比研究,采取石英-黄铁矿阶段样品4件,石英-多金属硫化物阶段样品5件进行测试。黄铁矿和方铅矿中流体包裹体中惰性气体同位素分析在核工业北京地质研究院分析测试研究所实验室完成,测试仪器采用的是HeliX SFT质谱仪,该仪器是美国赛默飞世尔(Thermo Fisher Scientific)公司最新一代分析惰性气体同位素组成的仪器。实验流程:粉碎并筛选出40~60目的样品,依次用乙醇、去离子水和丙酮超声清洗,除去样品表面吸附的杂质,设定温度为120 ℃烘干。烘干后,称取一定量的样品,放置压碎装置内,将装置全金属密封后在250 ℃条件下烘烤48 h,同时用无油分子泵组进行抽真空,除去压碎装置腔体及样品表面吸附气体。去气结束后,调用氦同位素测量离子源参数,并稳定30 min,依次测量整套系统本底值,标准氦气同位素组成值,压碎样品,对样品进行纯化并进行测量。HeliX SFT对He同位素的测定采用静态模式,用离子倍增器分别在4个时间段检测整套系统^{4}He的强度值,并计算系统本底的量。详细的测定过程参见李军杰等(2015)。

黄铁矿和方铅矿的硫同位素分析在核工业北京地质研究院分析测试研究中心完成。黄铁矿和方铅矿单矿物和氧化亚铜按1∶10研磨至200目左右,并混合均匀,在真空达2.0×10^{-2} Pa状态下加热,

图3 争光金矿矿石特征

a—石英黄铁矿网脉状矿石;b—浸染状黄铁矿脉石英型矿石;c—硅化绿帘石化角砾状矿石;d—面状黄铁矿石英型矿石;e—条带状石英闪锌矿黄铁矿矿石;f—块状黄铁矿方铅矿矿石;Py—黄铁矿;Qtz—石英;Ep—绿帘石;Sp—闪锌矿;Gn—方铅矿

Fig.3 Characteristics of ore in the Zhengguang gold deposit

a−Quartz pyrite reticulate vein ore; b−Dispersed pyrite gangue quartz type ore; c−Silicified epidote brecciated ore; d−Horizontal pyrite quartz type ore; e−Banded quartz sphalerite pyrite ore; f−The massive pyrite galena ore; Py−Pyrite; Qtz−Quartz; Ep−Epidote; Sp−Sphalerite; Gn−Galena

进行氧化反应,反应温度为980 ℃,生成二氧化硫气体在真空条件下,用冷冻法收集二氧化硫气体,并用MAT253气体同位素质谱分析硫同位素组成。测量结果以CDT为标准,记为$\delta^{34}S$。分析精度优于±0.2‰。硫化物参考标准为GBW-04414、GBW-04415硫化银标准,其$\delta^{34}S$分别是(-0.07±0.13)‰和(22.15±0.14)‰。

4　测试结果和讨论

4.1　He-Ar同位素

黄铁矿和方铅矿样品对氦同位素具有较好的保持能力,可反映原始地球内部流体的运移情况。黄铁矿和方铅矿发生漏气的程度远远小于其他矿物,流体包裹体被捕获后,寄主矿物黄铁矿晶格中由U、Th衰变所产生的放射成因^4He难以大量扩散进入流体包裹体,包裹体溶液中因U、Th含量很低,由其衰变而产生的^4He的量很少。压碎寄主矿物释放包裹体溶液的过程亦基本不会使寄主矿物中的^4He释放出来。此外,黄铁矿和方铅矿中钾的含量很低,因此钾的衰变也不可能生成较多的^{40}Ar。因此黄铁矿和方铅矿中流体包裹体的He和Ar同位素组成基本可以代表其成矿流体的氦氩同位素体系(Hu et al., 1998),可以用来广泛示踪金矿的成矿流体来源(Mao et al., 2002,2003;杨富全等,2006)。

争光金矿黄铁矿和方铅矿单矿物样品惰性气体同位素分析结果(表1)显示,黄铁矿各组分的含量分别为:$^4He=0.22\times10^{-7}$~2.98×10^{-7} cm^3STP/g,平均1.56×10^{-7} cm^3STP/g;$^{40}Ar=0.691\times10^{-7}$~$4.83\times10^{-7}$ cm^3STP/g,平均2.0×10^{-7} cm^3STP/g,R/Ra=1.08~3.59(R为样品中的$^3He/^4He$,Ra为大气中的$^3He/^4He$,Ra=1.4×10^{-6}),平均2.22;$^{40}Ar/^{36}Ar$=347.9~453.9,平均393.2。

热液流体中惰性气体主要有3种来源,且不同来源气体的氦、氩同位素组成及其特征比值具有显著差别(Burnard et al., 1999):(1)大气饱和水(ASW),$^3He/^4He$=1 Ra,$^{40}Ar/^{36}Ar$=295.5;(2)地幔流体,R/Ra值为6~9,$^{40}Ar/^{36}Ar$值变化较大,一般大于40000;(3)地壳流体,R/Ra值为0.01~0.05,而$^{40}Ar/^{36}Ar>295.5$。

黄铁矿和方铅矿流体包裹体分析测试过程中,大气对流体中氦的浓度的影响程度,可以根据参数F^4He来判断(Burnard et al., 1999)。F^4He为样品中$^4He/^{36}Ar$与大气$^4He/^{36}Ar$的比值(大气的$^4He/^{36}Ar$=0.1655)。假如样品中含有大气氦,则F^4He=1。争光矿床黄铁矿和方铅矿流体包裹体中F^4He远远大于1,有的高达4000余倍(表1)。因此,可以排除大气

表1　争光金矿黄铁矿和方铅矿流体包裹体He-Ar-S同位素组成

Table 1　Isotopic composition of He-Ar-S in fluid inclusions of pyrite and galena in Zhengguang gold deposit

样品编号	ZG01	ZG02	ZG03	ZG04	ZG05	ZG06	ZG07	ZG08	ZG09
测定矿物	黄铁矿	黄铁矿	黄铁矿	黄铁矿	黄铁矿	黄铁矿	黄铁矿	方铅矿	方铅矿
$^4He/(10^{-7}cm^3STP/g)$	1.32	1.16	0.22	0.992	2.98	2.05	1.53	1.37	2.44
$^3He/(10^{-13}cm^3STP/g)$	6.63	5.02	1.01	1.97	4.51	4.16	2.98	4.37	8.44
$^3He/^4He(R)$	5.03	4.33	4.59	1.99	1.51	2.03	1.95	3.19	3.46
$^{40}Ar/(10^{-7}cm^3STP/g)$	0.808	0.691	1.75	1.06	2.36	2.52	1.56	2.40	4.83
$^{40}Ar/^{36}Ar$	453.9±1.1	434.1±1.0	429.4±0.8	349.1±0.8	375.8±1.0	360.1±1.2	347.9±0.9	402.7±1.0	386.2±1.0
$^{40}Ar^*$	0.28	0.22	0.55	0.16	0.50	0.45	0.23	0.64	1.13
$^{40}Ar/^4He$	0.61	0.60	7.95	1.07	0.79	1.23	1.02	1.75	1.98
$^{40}Ar^*/^4He$	0.2136	0.1902	2.4805	0.1641	0.1692	0.2205	0.1536	0.4663	0.4649
$^{38}Ar/^{36}Ar$	0.198±0.002	0.193±0.003	0.196±0.002	0.198±0.002	0.189±0.002	0.193±0.002	0.198±0.003	0.189±0.002	0.191±0.002
^{36}Ar	0.00178	0.00159	0.00408	0.00304	0.00628	0.00700	0.00448	0.00596	0.01251
$^4He/^{36}Ar$	741.52	728.74	53.98	326.70	474.53	292.94	341.21	229.87	195.10
R/Ra	3.59±0.03	3.09±0.03	3.28±0.03	1.42±0.02	1.08±0.02	1.45±0.03	1.39±0.03	2.28±0.03	2.47±0.03
幔源He/%	45.63	39.25	41.62	17.94	13.57	18.31	17.58	28.87	31.33
$\delta^{34}S$	-2.6	-2.4	-1.8	-2.0	-2.1	-1.4	-1.2	-3.9	-3.6

注:$^{40}Ar^*$代表放射成因Ar。

对流体包裹体中氦的混染作用，表明黄铁矿和方铅矿流体包裹体中的氦氩同位素只可能来源于地慢和地壳。争光含金石英脉流体包裹体R/Ra=1.08~3.59，平均2.23，而$^{40}Ar/^{36}Ar$=347.9~453.9，平均393.2（表1），此数值远高于典型地壳流体，同时也反映出深源地幔流体的加入。

根据壳幔二元体系复合模式可计算样品中幔源氦加入的份额（徐永昌等, 1996）：幔源He(%)=(Rs−Rc)/(Rm−Rc)×100（Kendrick et al., 2001，其中Rs=样品值、Rm=8Ra、Rc=0.03Ra，分别代表样品、地幔、地壳流体的$^{3}He/^{4}He$比值），计算幔源He所占的比例为13.57%~45.63%，平均为28.23%（表1），说明成矿流体以地壳流体为主，并有幔源流体的加入。成矿流体的$^{40}Ar/^{4}He$比值集中于0.60~1.98，仅1个样品为7.95，明显高于地壳$^{40}Ar/^{4}He$生产比率（0.2）及地幔（0.33~0.56）流体（Stuart et al., 1995），样品全部落在地壳流体（C）和地幔流体（M）或地幔He和地壳He之间（图4，图5），显示地壳流体和地幔流体混合的特点。

4.2 硫同位素

争光金矿Ⅱ号矿体黄铁矿、方铅矿单矿物样品的硫同位素分析结果见表1。黄铁矿、方铅矿的$\delta^{34}S$值变化范围不大，为−1.2‰~−3.9‰，平均值−2.33‰，$\delta^{34}S$值黄铁矿大于方铅矿，显示体系硫同位素并未完全达到分馏平衡，但主体数据变化范围较窄，指示硫同位素分馏不强烈，也反映矿石硫源相对单一，具有深源岩浆硫同位素组成特征，该硫同位素组成与世界典型浅成低温热液型金矿床硫同位素$\delta^{34}S$值（0附近）（Heald, 1987）接近但稍偏负。前人研究显示，在较还原条件下，矿石中硫化物的$\delta^{34}S$组成与成矿流体的总S的硫同位素组成（$\sum\delta^{34}S$）基本一致（Ohmoto, 1972）。从争光金矿的矿石矿物组成看，其原生矿石主要由黄铁矿、闪锌矿、方铅矿等硫化物组成，未见硫酸盐矿物，流体包裹体中含较多碳氢化合物（邓珂等, 2013），显示其成矿流体处于较还原环境，因此含金石英脉中黄铁矿的$\delta^{34}S$组成基本可以代表成矿流体的总S硫同位素（$\sum\delta^{34}S$）组成。硫同位素主要有3个储存库，一是幔源硫（$\delta^{34}S$为−3‰~3‰，Chaussidon and Lorand, 1990），二是海水硫（$\delta^{34}S$为20‰左右），三是沉积物中还原硫，其硫同位素以具有较大的负值为特征（Rollinson, 1993）。争光金矿床的含金石英脉中黄铁矿、闪锌矿的$\delta^{34}S$值与幔源硫的值基本一致（表1），显示其成矿流体中的S可能部分来自深源地幔流体。

4.3 成矿机制

He−Ar−S同位素组成研究显示：争光金矿的成矿流体主要由地壳流体组成，但其中有地幔流体的加入。争光矿床石英脉中成矿流体的δD为−127‰~

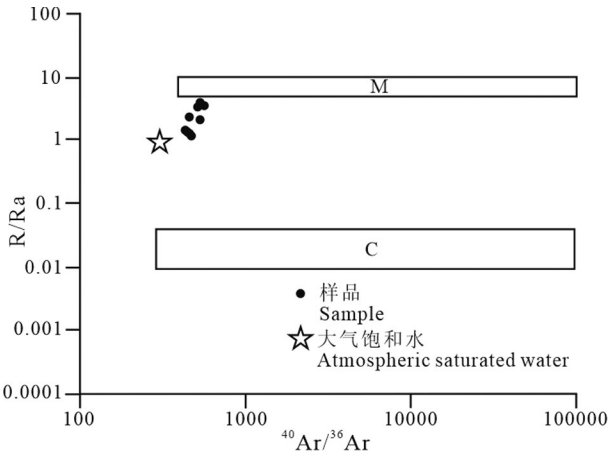

图4 黄铁矿流体包裹体$^{40}Ar/^{36}Ar$−R/Ra图（据Mamyrin and Tolstihkin, 1984修改）
M—地幔流体范围；C—地壳流体范围
Fig.4 $^{40}Ar/^{36}Ar$−R/Ra diagram of pyrite fluid inclusions (modified from Mamyrin and Tolstihkin, 1984)
M−Mantle fluid range; C−Crustal fluid range

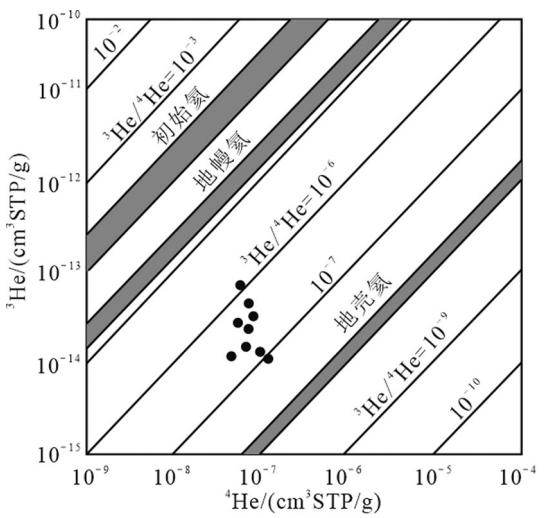

图5 黄铁矿流体包裹体$^{4}He-^{3}He$图（底图据Burnard et al., 1999修改）
Fig.5 $^{4}He-^{3}He$ of fluid inclusions in pyrite (modified from Burnard et al., 1999)

-110‰,$\delta^{18}O_{水}$为-5.9‰~0.6‰,显示大气降水与岩浆水的混合流体(车合伟等, 2016)。Gammons and Williams(1997)和John et al.(2003)认为,大气降水与围岩发生水岩反应时,可以同时萃取围岩中的Au和其他金属元素形成成矿流体。Heinrich et al.(2004)和Heinrich(2005)研究发现,岩浆侵位之后发生脱气作用,可以形成携带少量成矿物质的气相。

争光金矿床位于奥陶纪北东向多宝山岛弧带上,与多宝山—铜山铜钼矿床构成斑岩型-浅成低温热液型成矿系统,其成矿与早奥陶世(475 Ma)花岗闪长岩、闪长岩有关(郝宇杰,2015;李运等,2016;杨永胜等, 2016)。其成矿过程大致为:早中奥陶世,松嫩地块与兴安地块间洋壳向北俯冲(郝宇杰,2015;杨永胜等,2016),而俯冲流体交代地幔楔使其发生部分熔融,在兴安地块边缘形成早奥陶世多宝山火山岩岛弧(Wu et al., 2015),而熔体携带的Au、Cu等成矿元素在火山地层中产生预富集,而同受俯冲构造影响紧随多宝山火山岩的花岗质、闪长质岩浆的上侵定位不仅萃取了多宝山火山岩Au、Cu等元素,而且又携带了大量Au、Cu等成矿元素,含Au、Cu等元素的岩浆水沿断裂及构造破碎带运移到浅部有利构造位置时与下渗的大气降水混合形成成矿流体,由于温度和压力的下降和流体沸腾作用导致成矿流体物理化学条件的改变,从而使成矿物质沉淀,在次级断裂构造中形成含金硫化物石英网脉。

5 结　论

(1)争光金矿成矿流体的He和Ar同位素特征显示,成矿流体以壳源流体为主,并有幔源He的加入,幔源He的平均含量为28%,最高可达45%,幔源流体在成矿作用过程中起了重要的作用。

(2)幔源流体参与成矿表明,早奥陶世(~475 Ma)争光金矿是壳幔相互作用的结果。兴安地块与松嫩地块间的洋壳北西向俯冲,俯冲流体交代地幔楔发生部分熔融,形成大规模的玄武岩浆底侵或侵入地壳岩石,引起壳源岩浆产生,壳源岩浆热液与幔源岩浆结晶出的幔源流体以及大气水注入构造裂隙中以不同比例混合而形成争光金矿床。

References

Ballentine C J, Burgess R, Marty B. 2002. Tracing fluid origin, transport and interaction in the crust[J]. Reviews in Mineralogy and Geochemistry, 47: 539-614.

Burnard P G, Hu R Z, Turner G, Bi X W. 1999. Mantle, crustal and atmospheric noble gases in Ailaoshan gold deposits, Yunnan Province, China[J]. Geochimica et Cosmochimica Acta, 63: 1595-1604.

Chao Wenxin. 2018. Geological Characteristics and Genesis of Zhengguang Gold Deposit in Heihe City, Heilongjiang Province[D]. Changchun: Jilin University, 1-54 (in Chinese with English abstract).

Chaussidon M, Lorand J P. 1990. Sulphur isotope composition of orogenic spinel lherzolite massifs from Ariege (North- Eastern Pyrenees, France): An ion microprobe study[J]. Geochimica et Cosmochimica Acta, 54(10): 2835-2846.

Che Hewei, Zhou Zhenhua, Ma Xinghua, Ouyang Hegen, Liu Jun. 2016. Tentative discussion on genesis of Zhengguang Au deposit in northern Da Hinggan Mountains: Constrained by fluid inclusions and stable isotope composition[J]. Mineral Deposits, 35(3): 539-558 (in Chinese with English abstract).

Deng Ke, Li Nuo, Yang Yongfei, Zhang Cheng, Yu Yuanbang, Zhang Dongcai. 2013. Fluid inclusion constraints on the origin of the Zhengguang gold deposit, Heihe City, Heilongjiang Province [J]. Acta Petrologica Sinica, 29(1): 231-240 (in Chinese with English abstract).

Fu Yanli, Yang Yanchen. 2010. Deposit genesis and prospecting criteria of Zhengguang gold deposit, Heilongjiang[J]. Gold, 31(6): 13-18 (in Chinese with English abstract).

Gammons C H, Williams Jones A E. 1997. Chemical mobility of gold in the porphyry-epithermal environment[J]. Economic Geology, 92 (1): 45-59.

Gao Rongzhen, Lü Xinbiao, Yang Yongsheng, Li Chuncheng. 2015. Characteristics of cryptoexplosive breccias in the Zhengguang gold deposit of Heilongjiang Province and theirgeological implications[J]. Geology and Exploration, 50(5): 874- 883 (in Chinese with English abstract).

Hao Yujie. 2015. Mineralization and Metallogenic Regularity of Duobaoshan Ore Concentration Area in Heilongjiang Province, Northeast China[D]. Changchun: Jilin University, 1- 199 (in Chinese with English abstract).

Heald P, Foley N K, Hayba D O. 1987. Comparative anatomy of volcanic- hosted epithermal deposits acid- sulfate and adularia-sericite types[J]. Economic Geology, 80: 1-26.

Heilongjiang Qiqihar Mineral and Development Institute. 2009. Prospecting Report of Zhengguang Gold Deposit in Heihe City, Heilongjiang Province[R]. Heilongjiang Qiqihar Mineral and Development Institute, 82-116 (in Chinese).

Heinrich C A, Driesner T, Stefánsson A, Seward T M. 2004. Magmatic vapor contraction and the transport of gold from the porphyry environment to epithermal ore deposits[J]. Geology, 32(9): 761-764.

Heinrich C A. 2005. The physical and chemical evolution of low−salinity magmatic fluids at the porphyry to epithermal transition: A thermodynamic study[J]. Mineralium Deposita, 39: 864−889.

John D A, Hofstra A H, Fleck R J, Brummer J E, Saderholm E C. 2003. Geologic setting and genesis of the Mule Canyon low− sulfidation epithermal gold− silver deposit, North− Central Nevada[J]. Economic Geology, 98(2): 425−463.

Kendrick M A, Burgess R, Pattrick R A D, Turner G. 2001. Fluid inclusion noble gas and Halogen evidence on the origin of Cu−porphyry mineralizing fluids[J]. Geochimica et Cosmochimica Acta, 65(16): 2651−2668.

Li Junjie, Li Jian, Liu Hanbin, Zhang Jia, Jin Guishan, Zhang Jianfeng, Han Juan. 2015. Helium isotope composition of inclusions in mineral grains using Helix SFT Noble Gas Mass Spectrometer[J]. Acta Geologica Sinica, 89(10): 1826− 1831 (in Chinese with English abstract).

Li Yun, Fu Jiajun, Zhao Yuanyi, Zeng Hui. 2016. Chronological characteristics and metallogenic significance of Zhengguang gold deposit, Heilongjiang Province[J]. Acta Geologica Sinica, 90(1): 151−162 (in Chinese with English abstract).

Mamyrin B A, Tolstihkin I N. 1984. Helium Isotopes in Natures[M]. Amsterdam: Elsevier, 273.

Mao J W, Kerrich R, Li H Y. 2002. High $^{3}He/^{4}He$ ratios in the Wangu gold deposit, Hunan Province, China: Implications for mantle fluids along the Tanlu deep fault zone[J]. Geochemical Journal, 36: 197−208.

Mao J W, Li Y Q, Goldfarb R. 2003. Fluid inclusion and nobel gas studies of the Dongping gold deposit, Hebei Province: A mantle connection for mineralization[J]. Economic Geology, 98(3): 517−534.

Moreir M, Blusztajn J, Curtice J. 2003. He and Ne isotopes in oceanic crust: Implications for noble gas recycling in the mantle[J]. Earth and Planetary Science Letters, 216: 635−643.

Ohmoto H. 1972. Systematics of sulfur and carbon isotope in hydrothermal ore deposits[J]. Economic Geology, 67: 551−579.

Rollinson H R. 1993. Using Geochemical Data: Evaluation, Presentation, Interpretation[M]. London: Longman Scientific and Technical Press, 306−308.

Song Guoxue, Qin Kezhang, Wang Le, Gou Jihai, Li Zhenzhen, Tong Kuangyin, Zou Xinyu, Li Guangming. 2015. Type, zircon U− Pb age and Paleo volcano edifice of Zhengguang gold deposit in Duobaoshan ore field Heilongjiang Province, NE− China[J]. Acta Petrologica Sinica, 31(8): 2402− 2146 (in Chinese with English abstract).

Stuart F M, Burnard P, Taylor R P. 1995. Resolving mantle and crustal contributions to ancient hydrothermal fluid: He− Ar isotopes in fluid inclusions from Dae Hwa W− Mo mineralization, South Korea[J]. Geochimica et Cosmochimica Acta, 59: 4663−4673.

Sun Xiaoming, Xiong Dexin, Wang Shengwei, Shi Guiyong, Zhai Yong. 2006. Noble gases isotopic composition of fluid inclusions in scheelites collected from Daping gold mine, Yunnan Province, China, and its application for ore genesis[J]. Acta Petrologica Sinica, 22(3): 725−732 (in Chinese with English abstract).

Tong Kuangyin, Yang Yanchen, Song Gguoxue, Liang Haijun, Ma Longfei. 2015. Discussion on geological characteristics, ore genesis and prospecting of the Zhengguang Au− Zn deposit in Heilongjiang Province[J]. Geology and Exploration, 51(3): 507−518 (in Chinese with English abstract).

Winckler G, Aeschbach−Hertig W, Kipfer. 2001. Constraints on origin and evolution of red brines from helium and argon isotopes[J]. Earth and Planetary Science Letters, 184: 671−683.

Wu G, Chen Y C, Sun F Y. 2015. Geochronology, geochemistry, and Sr− Nd− Hf isotopes of the Early Paleozoic igneous rocks in the Duobaoshan area, NE China, and their geological significance[J]. Journal of Asian Earth Sciences, 97: 229−250.

Wu Ziyu, Sun Youcai, Wang Baoquan. 2006. Geology and geochemistry of Zhengguang gold deposit, Heilongjiang Province[J]. Geology and Prospecting, 42(1): 38− 842 (in Chinese with English abstract).

Xu Yongchang, Shen Ping, Tao Mingxin. 1996. Geochemistry of mantle− derived volatiles from natural gas in the eastern oil− gas Region. New types of helium Resources: Industrial reservoirs of mantle− derived helium in sedimentary crusts[J]. Science China (Series D), 26(1): 1−8 (in Chinese with English abstract).

Xue Chunji, Chen Yuchuan, Wang Denghong, Yang Jianmin, Yang Weiguang, Guan Ru. 2003. The Jinding and Baiyangping deposits, northwestern Yunnan: Geological feature, He, Ne and Xe isotope compositions, and metallogenic epoch[J]. Science in China, 33(4): 315−322 (in Chinese).

Yang Fuquan, Mao Jingwen, Wang Yitian, Zhao Caisgheng, Ye Hhuishou, Chen Wen. 2006. Chronology and geochemical characteristics of helium, argon, carbon and oxygen isotope in fluid inclusion of the Sawayaerdun gold deposit, Xinjiang, northwestern China and their significance[J]. Geological Review, 52(3): 341−351 (in Chinese with English abstract).

Yang Yongsheng, Lü Xinbiao, Gao Rongzhen, Li Chuncheng, Sun Xixin, Li Jie, Gun Minshan, Wu Jianliang, Xing Weiwei. 2016. Geochronology, geochemistry and geological significance of the tonalite porphyry in Zhengguang gold deposit, Heilongjiang Province[J]. Geotectonica et Metallogenia, 40(4): 674− 700 (in Chinese with English abstract).

Zeng Zhigang, Qin Yunshan, Zhai Shikui. 2001. He, Ne and Ar isotope compositions of nuid inclusions in hvdmthe Ⅱ llal sum des flrom the TAG hydmthe Ⅱ llal 6eld, Mid− Atlantic Ridge [J]. Science in China (series D), 30(6): 628−633 (in Chinese).

Zhao Guangjiagn, Hou Yushu, Cheng Fuqiang. 2007. Geological characteristics and genesis of Zhengguang gold deposit in Heihe City of Heilongjiang Province[J]. Nonferrous Metals, 59(3): 91−94

(in Chinese with English abstract).

Zhao Guangjiang, Hou Yushu, Wang Baoquan. 2006. Geological characteristics and genesis of Zhengguang gold deposit in Heilongjiang Province[J]. Non-Ferrous Mining and Metallurgy, 22(3): 3-6 (in Chinese with English abstract).

附中文参考文献

晁温馨. 2018. 黑龙江省黑河市争光金矿矿床地质特征及成因研究[D]. 长春: 吉林大学, 1-54.

车合伟, 周振华, 马星华, 欧阳荷根, 刘军. 2016. 大兴安岭北段争光金矿床成因探讨:来自流体包裹体及稳定同位素的制约[J]. 矿床地质, 35(3): 539-558.

邓轲, 李诺, 杨永飞, 张成, 于援帮, 张东财. 2013. 黑龙江省黑河市争光金矿流体包裹体研究及矿床成因[J]. 岩石学报, 29(1): 231-240.

付艳丽, 杨言辰. 2010. 黑龙江省争光金矿床成因及找矿标志[J]. 黄金, 31(6): 13-18.

高荣臻, 吕新彪, 杨永胜, 李春诚. 2015. 黑龙江争光金矿床隐爆角砾岩特征及其地质意义[J]. 地质与勘探, 50(5): 874-883.

郝宇杰. 2015. 黑龙江多宝山矿集区成矿作用与成矿规律研究[D]. 长春: 吉林大学, 1-199.

黑龙江省齐齐哈尔矿产勘察开发总院. 2009. 黑龙江省黑河市争光岩金矿勘探报告[R]. 黑龙江省齐齐哈尔矿产勘察开发总院, 82-116.

李军杰, 李剑, 刘汉彬, 张佳, 金贵善, 张建锋, 韩娟. 2015. Helix SFT惰性气体质谱仪分析矿物包裹体中氦同位素组成[J]. 地质学报, 89(10): 1826-1831.

李运, 符家骏, 赵元艺, 曾辉. 2016. 黑龙江争光金矿床年代学特征及成矿意义[J]. 地质学报, 90(1): 151-162.

宋国学, 秦克章, 王乐, 郭继海, 李真真, 佟匡胤, 邹心宇, 李光明. 2015. 黑龙江多宝山矿田争光金矿床类型、U-Pb年代学及古火山机构[J]. 岩石学报, 31(8): 2402-2416.

孙晓明, 熊德信, 王生伟, 石贵勇, 翟勇. 2006. 云南大坪金矿白钨矿惰性气体同位素组成及其成矿意义[J]. 岩石学报, 22(3): 725-732.

佟匡胤, 杨言辰, 宋国学, 梁海军, 马龙飞. 2015. 黑龙江争光金锌矿地质特征、矿床成因及找矿潜力探讨[J]. 地质与勘探, 51(3): 507-518.

武子玉, 孙有才, 王保全. 2006. 黑龙江争光金矿地质地球化学研究[J]. 地质与勘探, 42(1): 38-42.

徐永昌, 沈平, 陶明信. 1996. 东部油气区天然气中幔源挥发份的地球化学—Ⅰ. 氦资源的新类型: 沉积壳层幔源氦的工业储集[J]. 中国科学(D辑), 26(1): 1-8.

薛春纪, 陈毓川, 王登红, 杨建民, 杨伟光, 管荣. 2003. 滇西北金顶和白秧坪矿床地质和He, Ne, Xe同位素组成及成矿时代[J]. 中国科学(D辑), 33(4): 315-322.

杨富全, 毛景文, 王义天, 赵财胜, 叶会寿, 陈文. 2006. 新疆萨瓦亚尔顿金矿床年代学、氦氩碳氧同位素特征及其地质意义[J]. 地质论评, 52(3): 341-351.

杨永胜, 吕新彪, 高荣臻, 李春诚, 孙喜新, 李杰, 衮民汕, 吴建亮, 邢伟伟. 2016. 黑龙江争光金矿床英云闪长斑岩年代学、地球化学及地质意义[J]. 大地构造与成矿学, 40(4): 674-700.

曾志刚, 秦蕴珊, 翟世奎. 2000. 大西洋中脊TAG热液区硫化物中流体包裹体的He-Ne-Ar同位素组成[J]. 中国科学(D辑), 30(6): 628-633.

赵广江, 候玉树, 程富强. 2007. 黑龙江黑河市争光岩金矿床地质特征及成因浅析[J]. 有色金属, 59(3): 91-94.

赵广江, 侯玉树, 王宝权. 2006. 黑龙江省争光金矿地质特征及成因初探[J]. 有色矿冶, 22(3): 3-6.